On the numerical asymmetry in calculating Coriolis terms through the splitting method in a mesoscale model

Pinhas Alpert*

Raymond and Beverly Sackler Faculty of Exact Sciences,
Department of Geophysics and Planetary Sciences,
Tel Aviv University,
Tel Aviv 69978, Israel
Fax: +972-3-640-9282
E-mail: pinhas@cyclone.tau.ac.il
*Corresponding author

Hannu Savijärvi

Division of Atmospheric Sciences,
Department of Physical Sciences,
FIN-00014 University of Helsinki,
P.O. Box 64, Helsinki, Finland
Fax: +358-9-191-57860
E-mail: hannu.savijarvi@helsinki.fi

Abstract: The asymmetry in calculating the Coriolis terms by Marchuk's splitting method is discussed. It was found that although some asymmetry is required for linear stability, this asymmetry should be kept to a minimum. Otherwise, for instance, if the diffusion terms are calculated in between the Coriolis terms in the u and v equations of motion, one gets cross-isobaric low-level winds, which are different depending on the geostrophic wind direction. This is the first study to show that the required asymmetry in the splitting can cause a considerable error in the boundary-layer winds of atmospheric models if not handled in a specific way.

Keywords: splitting method; mesoscale model; Ekman spiral.

Reference to this paper should be made as follows: Alpert, P. and Savijärvi, H. (2008) 'On the numerical asymmetry in calculating Coriolis terms through the splitting method in a mesoscale model', *Int. J. Environment and Pollution*, Vol. 32, No. 2, pp.139–148.

Biographical notes: Pinhas Alpert is a Developer of a novel Factor Separation Method in numerical simulations (Stein/Alpert, JAS 1993), and it is now adapted by groups worldwide with numerous publications. He is a coauthor of more than 120 peer-reviewed papers mainly on aspects of mesoscale dynamics and climate. His areas of research focus on atmospheric dynamics, climatology, numerical methods, limited area modelling and climatic change. The core atmospheric model developed during his PhD (1980) was extended and is currently used in Belgium (LLN) and Finland (UH).

Hannu Savijärvi is a Professor of Meteorology at the University of Helsinki, since 1997. Previously, he worked at ECMWF, NCEP and GFDL as a visiting scientist. His areas of interest are in numerical modelling of planetary atmospheres in all scales and especially at the mesoscale. He pioneered mesoscale and boundary layer modelling for planet Mars, and has developed for example, the radiation scheme now being used in the North European operational weather forecast model HIRLAM..

1 Introduction

Mesoscale models are becoming a common tool in mesoscale research and in local forecasting. Quite a few of the existing or projected models use the so-called 'splitting' method, suggested by Marchuk (1974), where the time integration of the physically different terms is split into several parts. The purpose of this paper is to show that although some asymmetry is necessary in applying the Coriolis terms with the splitting method, to avoid linearly unstable solutions (Pielke, 1984, p.290), this asymmetry must be kept to a minimum. To the best of our knowledge, this paper is the first to point out that the required asymmetry can cause a considerable error if not handled in a particular way of splitting.

The experiments were made when implementing a two-dimensional mesoscale model (Alpert et al., 1982) in the Department of Meteorology, University of Helsinki, for further use in localised mesoscale studies. The asymmetry was minimised in the numerical scheme. As a result, the asymmetry in the model results was completely removed in idealised Ekman layer simulations where comparison can be made to an analytic solution.

The modified Alpert et al. (1982) model, equipped with good-quality parameterisations developed in the University of Helsinki (and documented in the below-mentioned references), has been used, for example, for studies about coastal convergence (Alestalo and Savijärvi, 1985), coastal winds (Savijärvi, 2004), sea breezes (Neumann and Savijärvi, 1986; Savijärvi, 1995, 1997; Savijärvi and Alestalo, 1988), slope winds and low-level jets (Savijärvi, 1991), urban heat island circulations (Savijärvi, 1985; Savijärvi and Jin, 2001), tropical heat islands (Savijärvi and Matthews, 2004), surface heterogeneities (Savijärvi and Amnell, 2001; Vihma and Savijärvi, 1991), coastal low-level jets (Savijärvi et al., 2005) and Arctic flows (Vihma and Brmmer, 2002). There is even a version for planet Mars (Savijärvi, 1999; Savijärvi and Siili, 1993; Siili et al., 1999). In all cases, the modified model has produced local winds, which have been close to the available observations.

2 The original model and Ekman layer simulation

This model is dry, hydrostatic and two-dimensional in a terrain-following x-sigma coordinate system. It uses the K-theory for turbulence and assumes a steady, large-scale background pressure field in a form of geostrophic wind. The surface roughness, topography and temperature are specified. The model equations, numerical methods and boundary conditions are described in detail in Alpert et al. (1982) and in the references therein. Therefore, only a brief review is given here.

The model grid length is 4 km and there are 10 levels with approximate heights of 10, 20, 35, 60, 110, 190, 350, 600, 1100 and 2000 m. The flow follows the ground ($P_s \approx 1000$ mb) and top level ($P_t = 750$ mb). Turbulent fluxes vanish at the upper boundary and all horizontal gradients vanish in the lateral boundaries. Vertical diffusion is calculated with an implicit method and horizontal advection is based on a cubic spline upstream interpolation. Instead of explicit horizontal diffusion, a selective low-pass filter is applied horizontally for each variable.

The time integration scheme of this model is based on Marchuk splitting, which essentially means that the individual tendencies given by various terms in the predictive equations are used to update the fields immediately so that the scheme becomes in some senses implicit for the last terms. This enhances numerical stability. Figure 1 lists the terms for the primitive equations of motion in the model and the original time integration methods for each term. Note that in the original model schemes, the Coriolis force term fv and the large-scale pressure gradient force $-fv_g$ are calculated, and the u-field is updated, before the respective terms for the u-field, and also before the calculation of the vertical diffusion terms. This makes the scheme somewhat asymmetric with respect to the accuracy wind components are being calculated, but prevents the solutions from being linearly unstable, if $|f\Delta t| < 2$, (see e.g. Pielke, 1984, p.290). This condition is not a practical restriction, as it is fulfilled, for example, at 60°N, for time steps of up to 4.3 hr.

To test this numerical scheme, the original model was applied to the idealised Ekman spiral conditions, then the analytic solution is being known exactly. Thus, the topography was set flat, the initial lapse rate was set neutral, vertically constant geostrophic wind was applied and the turbulent diffusivity K_Z was set constant, $K_Z = 5$ m^2/s, at all levels including the lowest 10-m level. These conditions make the model essentially one-dimensional, as no horizontal gradients are produced during the time integration. Thus, there is no horizontal convergence and vertical motion and the temperature and height distributions remain at their initial values.

Figure 1 The time integration schemes for the terms in the equations of motion in the original model. Each field is updated before applying the next term. The suggested modification is indicated by an arrow

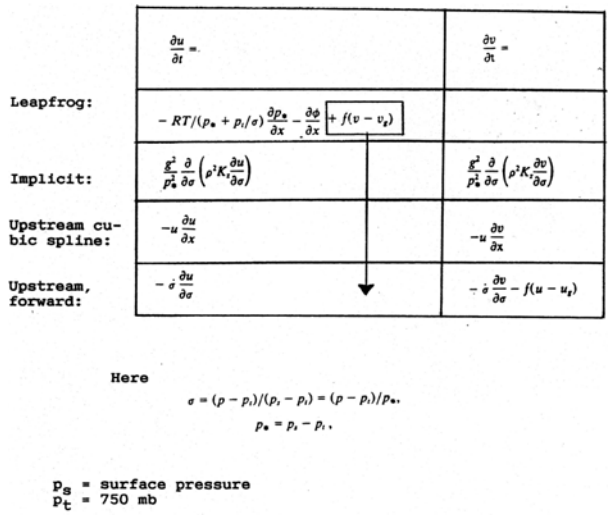

By setting the wind to non-zero initially, and time integrating, the only non-zero terms in the model equations become under these conditions

$$\frac{\partial u}{\partial t} = -f(v - v_g) + K_Z \frac{\partial^2 u}{\partial z^2}; \qquad \frac{\partial v}{\partial t} = -f(u - u_g) + K_Z \frac{\partial^2 v}{\partial z^2} \tag{1}$$

that describe frictionally damped inertial oscillation towards a steady state. The analytic solution to the steady state is obviously the Ekman spiral. The model integrations are shown in Figures 2 and 3, initial wind being here the geostrophic wind will be at all heights. Figure 2 shows the time evolution of the v component at the 190-m level in the case $(u_g, v_g) = (0, 10)$ m/s. Figure 3 shows wind hodographs at 4, 8, 12 and 16 hr after start for two orientations of a geostrophic wind of 10 m/s, together with the analytic solution at 60°N. The wind height hodograph is a convenient way to present the change of the wind velocity vector as a function of height. Thus, the points on the curves in Figure 3 correspond to u and v solutions for specific model height levels. The arrows illustrate the time evolution of the wind vector end point at some specific heights as the integration goes on.

Figure 2 The time evolution of v-component in the original model at level 5 (190 m); $(u_g, v_g) = (0, 10)$ m/s

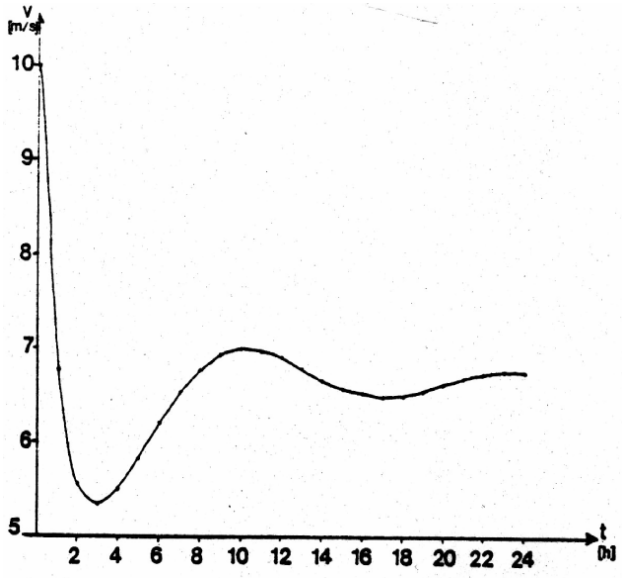

The integrations exhibit frictionally damped inertial oscillation and a quasi-steady state is reached in about 16 hr. What is peculiar in this steady state is that with the geostrophic wind in the x-direction (Figure. 3(a)), the model is underestimating the cross-isobaric wind component, but with the geostrophic wind in the y-direction (Figure 3(b)), the cross-isobaric wind is overestimated. The induced cross-isobaric mass transport varies thus by a factor of 2, for the same K_Z, depending on the geostrophic wind direction. This is clearly wrong.

Figure 3 (a) The wind hodograph in the Ekman solution at 60°N (thin line) and in the original model at 4, 8, 12 and 16 hr after start; $(u_g, v_g) = (10, 0)$ m/s, $K_Z = 5\text{m}^2/\text{s}$ and (b) same as (a) but for $(u_g, v_g) = (0, 10)$ m/s

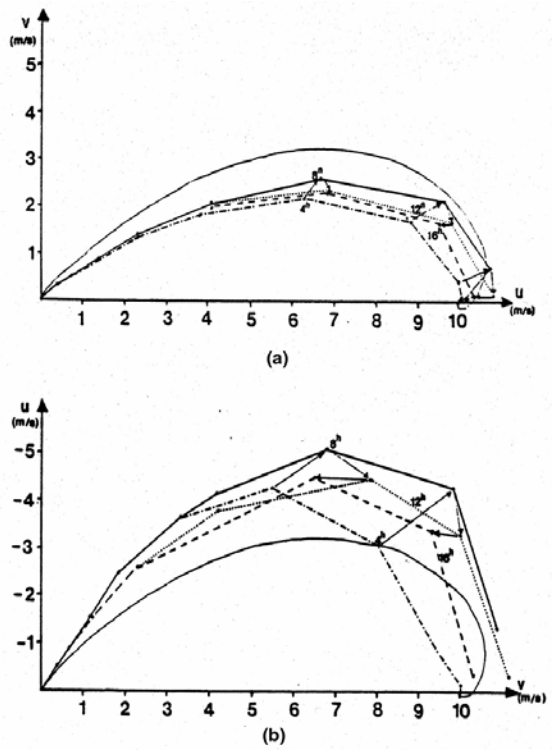

3 The modified model

The reason for the asymmetry in the original model results described in Section 2 was thought to be the asymmetry in the model code referred to in the description of the split time integration method. Accordingly, the numerical scheme was made less asymmetric by calculating the Coriolis force components consecutively at the same stage, as indicated in Figure 1. At the same time, the leapfrog scheme ($u^{n+1} = u^{n-1} + 2\Delta t f^n$ for $du/dt = f$) was changed to the Adams-Bashworth scheme ($u^{n+1} = u^n + \Delta t(1.5f^n - 0.5f^{n-1})$) for the pressure gradient force in the u-equation of motion. This change was made because of the fact that in case of weak or no mesoscale pressure gradient forcing (such as in the present Ekman simulations), the later stages of the split calculations would effectively use values of u^{n-1} instead of u^n as the latest values of u. The damping of the computational mode in the Adams-Bashworth scheme was considered as extra benefit, although it is acknowledged that this method is slightly less accurate than the leapfrog scheme.

With these modifications, the results shown in Figure 4 are much better and an accurate Ekman spiral is achieved in 16 hr independent of the geostrophic wind direction. (Note that the initial wind in Figures 2–4 is quite far from the final steady

state). The minimised asymmetry in the modified scheme, which is necessary for the numerical stability of the Coriolis terms, might even be unnecessary in a fully non-linear and diffusive model because the linear instability is not quite effective in the presence of realistic diffusion.

Figure 4 Same as Figure 3 but for the modified model

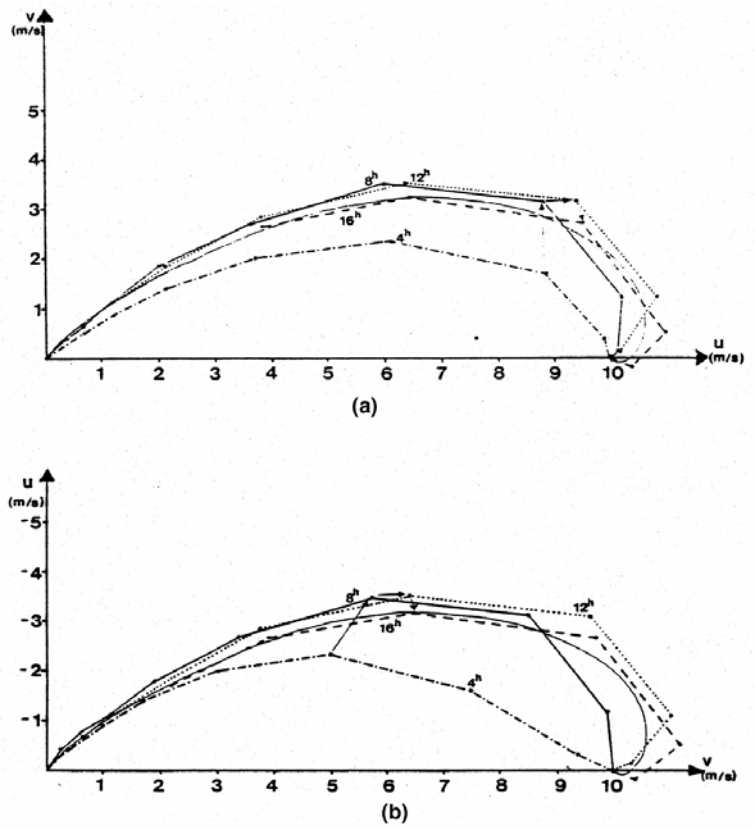

4 Further comparisons and discussion

An important question is whether our results are just a direct consequence of the specific numerical schemes that we have used. A partial answer was given by the experiments described in the following that have been independently performed by Y. Mahrer (personal communication) with the quite different Pielke-Mahrer's model. They have revealed similar features. Five experiments were performed in which realistic (non-constant) *K*-profiles were assumed. In the following the upper indices n and $n + 1$ indicate the older and the updated values, respectively:

1 v^n was employed in calculating u^{n+1} by the finite difference approximation for Equation (1), and u^{n+1} in calculating v^{n+1}; both were calculated consecutively after diffusion (as in this modified model). $(u_g, v_g) = (0, 10)$ m/s.

2 Same as step 1 but $(u_g, v_g) = (10, 0)$ m/s.

3 v^n in calculating u^{n+1} and u^n in calculating v^{n+1} $(u_g, v_g) = (0, 10)$ m/s.

4 Same as step 3 but $(u_g, v_g) = (10, 0)$ m/s.

5 v^n in calculating u^{n+1} before diffusion and u^{n+1} in calculating v^{n+1} but after diffusion (as in this original model). $(u_g, v_g) = (0, 10)$ m/s.

Steady-state results were obtained after 16 hr of simulation. The following conclusions were derived from them:

- (1) and (2) give identical results (differences less than 0.1%)
- (3) and (4) give nearly identical results (differences less than 1%) and
- (1) and (5) give different results (differences greater than 15%).

As an example, the five lowest steady-state cross-isobaric wind components for the cases (1) and (5) are:

	Height(m)	*5*	*15*	*200*	*100*	*300*
Exp. (1)	u(m/s)	–1.629	–1.546	–1.608	–1.241	–1.537
Exp. (5)	u(m/s)	–1.704	–1.563	–1.750	–1.463	–1.721

Experiments (1) and (5) resemble the modified and original model runs, respectively. The analogous differences in these experiments (Figures 4(b) and 3(b), respectively) were 30–40%, but this is to be expected as the intensities of the Ekman cross-isobaric winds are much larger, due to constant K_Z. This also suggests that the asymmetry has a weaker effect with realistic non-constant *K*-profiles. Furthermore, it is expected that the effect will be even more reduced in a full-mesoscale modelling, which includes a strong forcing and significant horizontal diffusion.

It should be stressed following the aforementioned experiments that the asymmetry effect in the calculation of the Coriolis terms becomes significant only in the case where the diffusion terms are being calculated between the two Coriolis terms – see Figure 1 and experiment (5).

5 The modified model wind profile with variable diffusion

The Ekman profile is never observed in the atmosphere because (among the other good reasons) K_Z is not constant near the surface. For comparison, Figure 5(a) shows the steady-state wind hodograph in this modified model after K_Z is made flow-dependent by using the standard Prandtl (Blackadar, 1978) formulation

$$K_Z = l^2 \left| \frac{\partial \vec{V}}{\partial z} \right|; \quad l = \frac{kz}{(1 + kz/\lambda)}; \quad k = 0.4, \ \lambda = 40\,\mathrm{m}$$

except in the lowest $h = 10$ m level where the drag law is used:

$$\vec{\tau}_h = \rho_h c_d \left|\vec{V}_h\right| \vec{V}_h; \quad c_d = \left(\frac{k}{l\mathrm{n}(h/z_0)}\right)^2$$

No heating, flat topography and neutral stratification are assumed. The results with $z_0 = 10$ cm and $z_0 = 1$ mm are labelled land and sea, respectively. The 'land' wind hodograph is quite similar to the observed classical Leipzig wind profile (e.g. Lettau, 1950) especially near the ground, where the model resolution is high. The Leipzig profile was observed in a strong, steady, slightly stable flow in a well-developed cyclone. The K_z profile of the model steady state is shown in Figure 5(b) indicating a maximum K_z at about 300 m. It is also similar to that from the Leipzig profile.

Figure 5 (a) The wind hodograph in the Ekman solution at 60°N and in the steady state of the modified model with variable K_z. The 10 m wind is drawn as an arrow. Land and sea refer to z_0 values of 10 cm and 1 mm, respectively and (b) the K_z profile over land

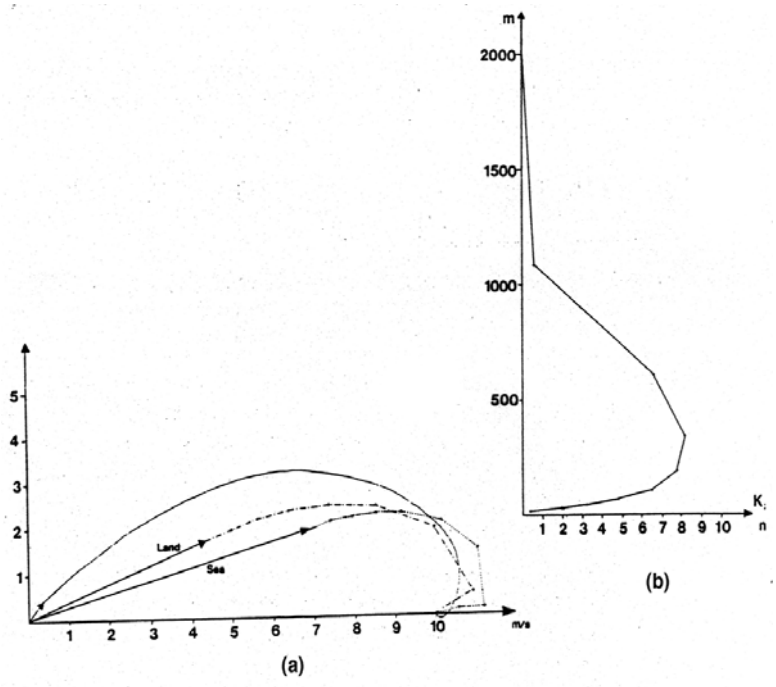

6 Conclusion

The asymmetry in calculating the Coriolis terms by Marchuk's splitting method is discussed. It was found that although some asymmetry is required for linear stability, this asymmetry should be kept to a minimum. Otherwise, for instance, if the diffusion terms are calculated in between the Coriolis terms in the u and v equations of motion, one gets cross-isobaric low-level winds, which are different depending on the geostrophic wind direction.

Acknowledgements

We are grateful to the late Jehuda Neumann and Mikko Alestalo for their advice and substantial help in initiating the experiments. Special thanks are due to Ytzhak Mahrer for the performance of the calculations with the Pielke-Mahrer model during his stay at the Cooperative Institute for Research in the Atmosphere (CIRA), CSU/NOAA. This research was supported by a grant (GLOWA – Jordan River) from the German Bundesministerium fuer Bildung und Forschung (BMBF) and the Israeli Ministry of Science and Technology (MOST). We thank Haim Shafir for typing the manuscript.

References

Alestalo, M. and Savijärvi, H. (1985) 'Mesoscale circulations in a hydrostatic model: coastal convergence and orographic lifting', *Tellus*, Vol. 37A, pp.156–162.

Alpert, P., Cohen, A., Neumann, J. and Doron, E. (1982) 'A model simulation of the summer circulation from the Eastern Mediterranean past Lake Kinneret in the Jordan Valley', *Monthly Weather Review*, Vol. 110, pp.994–1006.

Blackadar, A.K. (1978) 'High resolution models of the planetary boundary layer', *Advances in Environmental and Scientific Engineering*, Gordon and Breach, Vol. 1, p.176.

Lettau, H. (1950) 'A reexamination of the Leipzig wind profile considering some relations between wind and turbulence in the frictional layer', *Tellus*, Vol. 2, pp.125–129.

Marchuk, G.I. (1974) *Numerical Methods in Weather Prediction*, Academic Press, p.277.

Neumann, J. and Savijärvi, H. (1986) 'The sea breeze on a steep coast', *Beitraege zur Physik der Atmosphaere*, Vol. 59, pp.375–389.

Pielke, R.A. (1984) *Mesoscale Meteorological Modelling*, Academic Press, p.612.

Savijärvi, H. (1985) 'The sea breeze and urban heat island circulation in a numerical model', *Geophysica*, Vol. 21, pp.115–126.

Savijärvi, H. (1991) 'The US great plains diurnal ABL variation and the nocturnal low-level jet', *Monthly Weather Review*, Vol. 119, pp.833–840.

Savijärvi, H. (1995) 'Sea breeze effects on large-scale atmospheric flow', *Contributions to Atmospheric Physics*, Vol. 68, pp.335–344.

Savijärvi, H. (1997) 'Diurnal winds around Lake Tanganyika', *Quarterly Journal of the Royal Meteorological Society*, Vol. 123, pp.883–899.

Savijärvi, H. (1999) 'A model study of the atmospheric boundary layer in the Mars Pathfinder conditions', *Quarterly Journal of the Royal Meteorological Society*, Vol. 125, pp.483–493.

Savijärvi, H. (2004) 'Model predictions of coastal winds in a small scale', *Tellus*, Vol. 56A, pp.287–295.

Savijärvi, H. and Alestalo, M. (1988) 'The sea breeze over a lake or gulf as the function of prevailing flow', *Contributions to Atmospheric Physics*, Vol. 61, pp.98–104.

Savijärvi, H. and Amnell, T. (2001) 'High-resolution flight observations and numerical simulations: horizontal variability in the wintertime boreal boundary layer', *Theoretical and Applied Climatology*, Vol. 70, pp.245–252.

Savijärvi, H. and Jin, L. (2001) 'Local winds in a valley city', *Boundary-Layer Meteorology*, Vol. 100, pp.301–319.

Savijärvi, H. and Matthews, S. (2004) 'Flow over small heat islands: a numerical sensitivity study', *Journal of Atmospheric Science*, Vol. 61, pp.859–868.

Savijärvi, H., Niemel, S. and Tisler, P. (2005) 'Coastal winds and low-level jets: simulations for sea gulfs', *Quarterly Journal of the Royal Meteorological Society*, Vol. 131, pp.625–637.

Savijärvi, H. and Siili, T. (1993) 'The Martian slope winds and the nocturnal PBL jet', *Journal of Atmospheric Science*, Vol. 50, pp.77–88.

Siili, T., Murphy, J., Haberle, R. and Savijärvi, H. (1999) 'Modelling of the combined late-winter ice cap and slope winds in Mars' Hellas and Argyre regions', *Planetary Space Science*, Vol. 47, pp.951–970.

Vihma, T. and Brmmer, B. (2002) 'Observations and modelling of on-ice and off-ice air flows over the northern Baltic Sea', *Boundary-Layer Meteorology*, Vol. 103, pp.1–27.

Vihma, T. and Savijärvi, H. (1991) 'On the effective roughness length over heterogeneous terrain', *Quarterly Journal of the Royal Meteorological Society*, Vol. 117, pp.399–408.